17th World Conference on Earthquake Engineering, 17WCEE
Sendai, Japan - September 13th to 18th 2020

PUSHOVER BASED TORSIONAL RESPONSE OF INFILL WALL BUILDINGS WITH PLAN AND VERTICAL IRREGULARITIES

S.C. Mohan [(1)], CH.B.V. Hareen [(2)]

[(1)] *Asst. Professor, Department of Civil Engineering, BITS Pilani Hyderabad Campus, Hyderabad-500 078, Telangana, India, mohansc@hyderabad.bits-pilani.ac.in*
[(2)] *Research scholar, Department of Civil Engineering, BITS Pilani Hyderabad Campus, Hyderabad-500 078, Telangana, India, P20160404@hyderabad.bits-pilani.ac.in*

Abstract

Interaction between masonry infill wall and surrounding RC frame alters the lateral load path of buildings subjected to ground motion. In the existing literature, few studies addressed torsional response of plan symmetric RC buildings with asymmetric distribution of infill walls. With the help of advanced modeling techniques, this study investigates the inelastic torsional response of multistory RC infill wall buildings with vertical and plan irregularities. Nonlinear modeling of plan asymmetric buildings was carried out in SeismoStruct 2016 software using force-based fibre beam-column elements. Pushover analysis is performed on the buildings, which involves a double strut macro-model for infill walls. The torsional response of the buildings obtained from Extended N2 method and Extended Capacity Spectrum Method –FEMA 440 is presented. The response parameters considered are Story Drift Ratio (SDR) and demand to capacity ratio (D/C) of column curvature at stiff, flexible side of the buildings. Compared to bare frame building, the SDR and D/C ratio of bottom story columns is higher at the flexible side and moderately higher near stiff side for building with infill walls. Infill wall interaction has led to the modification of torsional response by increasing the vulnerability of flexible side column to damage in vertically regular and irregular buildings.

Keywords: Plan asymmetric building; vertical stiffness irregularity; masonry infills; pushover analysis; torsional response

1. Introduction

Eccentricity in the floor plan of a building will cause uneven distribution of lateral forces to the peripheral frames. This distribution induces an excessive edge deformation leading to failure of brittle and non-ductile elements situated at the edges. The failure of these elements may result in a sudden loss of the building's strength and stiffness. The seismic torsional response of plan asymmetric multistory buildings is widely studied. In the majority of those studies, the infill wall interaction with frame is grossly ignored. Even in plan symmetric buildings, stiffness eccentricity can be observed when infill walls are distributed asymmetrically in plan. In the case of building with three adjacent sides infilled, the global seismic performance of the building was significantly affected due to localized deformations in the beams and columns near flexible side under higher levels of excitation [1]. The effect of asymmetric infill wall distribution on the torsional response of plan symmetric RC buildings was further investigated experimentally [2] and numerically [3]. The seismic damage reported for building with infill walls on two adjacent sides is found to be higher compared to the case of symmetric distribution of infill walls in the plan. This damage also depends on the magnitude of eccentricity arising from irregular distribution infill walls.

Limited studies addressed the seismic response of asymmetric buildings with infill walls and vertical stiffness irregularity [4,5]. These studies concluded that buildings with bare frames are more susceptible to damage compared to infill wall buildings. However, these studies do not highlight the modification in the torsional response due to infill walls in asymmetric plan buildings.

Typically, the seismic design of a symmetric or asymmetric building involves analysis for lateral loads to attain stiffness and strength characteristics. In this process, infill wall stiffness is generally not considered. However, the interaction between the infill wall and surrounding RC frame alters the lateral load path of buildings subjected to ground motion. Therefore, a study on the collapse behavior of buildings with infill walls is necessary to suggest suitable measures for designers to prevent significant loss of strength and stiffness of lateral load resisting elements. Hence, this study primarily investigates the torsional response of plan asymmetric buildings with infill walls distributed uniformly in the plan. This study also examined the influence of vertical stiffness irregularity on the torsional response of plan asymmetric infill wall buildings.

2. Modeling and Design

A total of seven plan asymmetric multistory RC buildings are considered for the study. Asymmetric distribution of shear walls in plan gives rise to stiffness eccentricity on all floors. The buildings are resting on medium type soil (10 < *Standard Penetration Test (N)* < 30) and located in Zone III ($PGA = 0.16g$) of Indian seismicity, except the building shown in Fig. 1(d) located in Zone IV ($PGA = 0.24g$). The increase of bottom story height compared to the above story lead to vertical stiffness irregularity (VSI), whereas for buildings without (w/o) VSI the story height is similar. The thickness of RC slab is set to 115 mm, which is supposed to withstand Live Load of 2.0 kN/m^2 and Floor finish 1.5 kN/m^2. The response reduction factor (R) is taken as 5 for all the cases, which represents buildings with special moment resisting frames. The importance factor considered is 1.0, since the buildings are dwelling units. Analysis of buildings under combined gravity and lateral loads is carried out using STAAD.ProV8*i* (*SELECTseries4™*) confirming to IS 1893 standard [6]. The lateral forces required for design are arrived using linear dynamic analysis under design basis earthquake. Concrete of grade M30 is adopted for L, T & U shape buildings, and M25 grade for the remaining buildings. Grade of steel considered is Fe500 for all buildings. The design of beams, columns, and shear walls confirm to IS 13920:2016, IS 456:2000 codal provisions. The plan of the asymmetric buildings is depicted in Fig.1, which includes the center of mass(CM) and center of rigidity(CR) locations of the first floor. The rectangular building shown in Fig.1(d) is of G+3 Upper Floors, and the typical elevation of the buildings is shown in Fig.1(h).

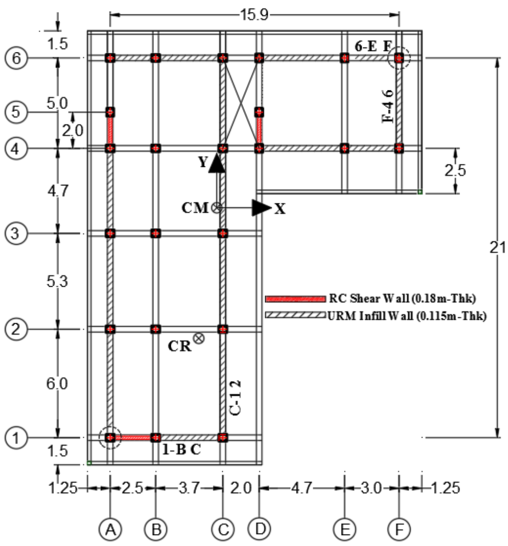

(a) L Building

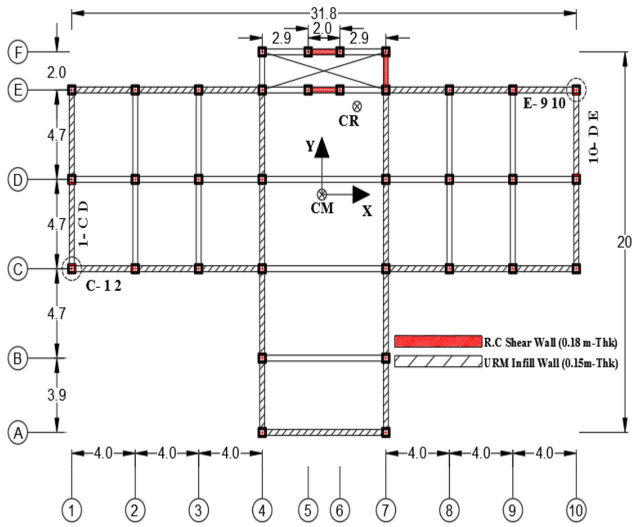

(b) T Building

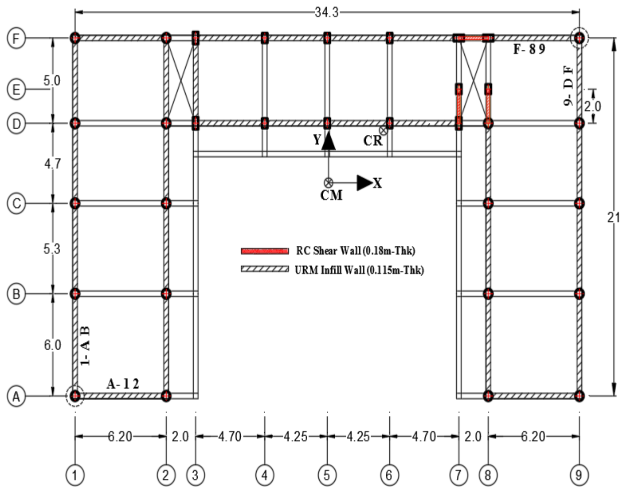

(c) U Building

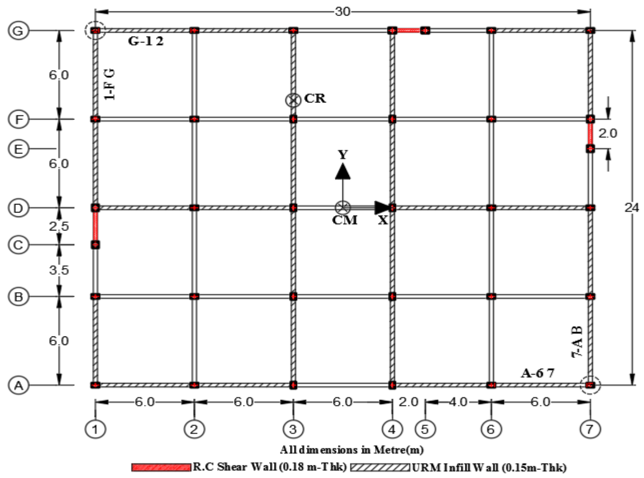

(d) R Building-3P (3 Peripheral shear walls)

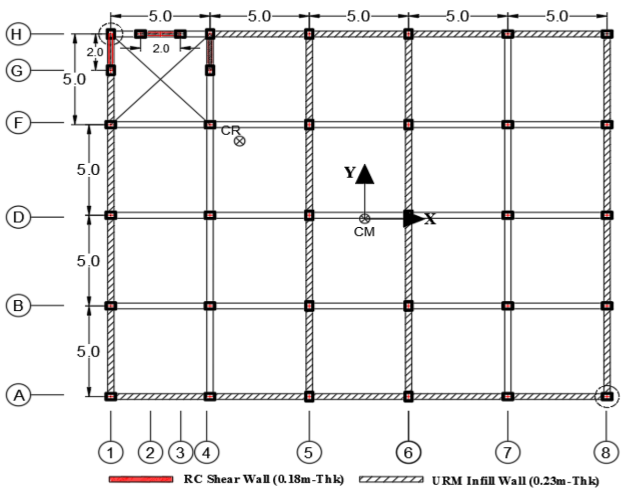

(e) R Building-C (Corner shear walls)

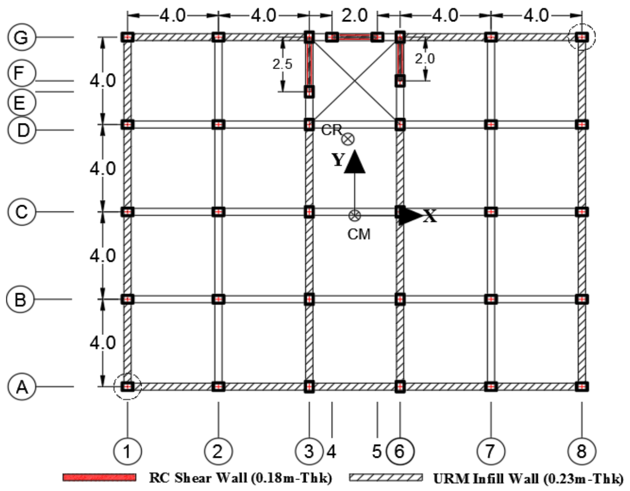

(f) R Building-M (Middle shear walls)

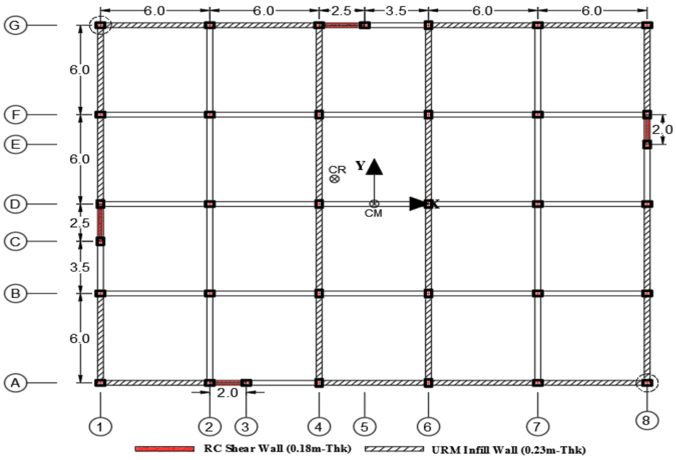

(g) R Building-4P (4 Peripheral shear walls)

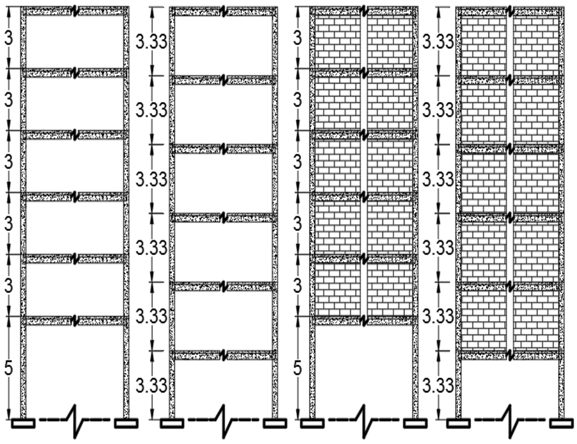

(h) Typical elevation of VSI and w/o VSI buildings

Fig. 1 – Plan and elevation of multistory plan asymmetric RC buildings

2.1 Nonlinear modeling and analysis

Plan asymmetric RC buildings are modeled and analyzed using SeismoStruct 2016, a fibre based finite element software [7]. The nonlinear behavior of concrete compression and reinforcement bars are modeled using Mander et al. [8], Monti-Nuti [9] models, respectively. With these material models, the ultimate strain in confined concrete for beam and column is evaluated utilizing a computer program CONSEC© [10]. The crushing strain of unconfined concrete is set to 0.0035 followed by a spalling strain of 0.005 for all beams and columns.

2.1.1 Fibre Element

Beams and columns are modeled using force-based concentrated plastic hinge frame elements. The plastic hinge length (L_p) is taken as half the section depth [11]. For shear wall, a force-based distributed inelasticity frame element is adopted. By default, two integration sections will be considered for plastic hinge elements, whereas for distributed inelasticity elements, five integration sections are defined. For columns and shear wall axial load bending moment interaction is inherently accounted.

2.1.2 Rigid diaphragm

Rigid diaphragm effect is modeled for the slabs of RC buildings through penalty functions nodal constraints approach. The penalty function exponent suitable to the model is arrived on an iteration basis [12]. Penalty function exponent is taken as 10^5 for rectangular building and 10^7 for remaining buildings.

2.1.3 Infill Wall

Unreinforced masonry(URM) infill walls are modeled using a macro-model approach proposed by Crisafulli and Carr [13]. This macro model is shown in Fig.2 accounts compression, shear behavior of infill panels with the help of two parallel struts and a shear spring, respectively. The geometrical properties of compression and shear strut are calculated according to the stipulations provided in IS 1893 and SeismoStruct 2016 software user manual. Infill walls are composed of burnt clay red bricks with two different mortar compostions, i.e., cement, lime, and sand (1:0.5:4.5) for Rectangular, L T, and U shape buildings and 1:0:6 for the remaining buildings. The density of clay brick is 18 kN/m^3, with a compressive strength of 3.5 MPa (IS: 1077-2007). For mortar, the compressive strength values are taken to be 6 MPa (1:0.5:4.5), 3 MPa (1:0:6) as per IS: 1905-2002. The stress-strain curve for masonry prism with selected mortar composition is obtained from analytical expression developed based on experimental studies [14]. The stress-strain curve for masonry prisms with different grades of mortar is shown in Fig.3.

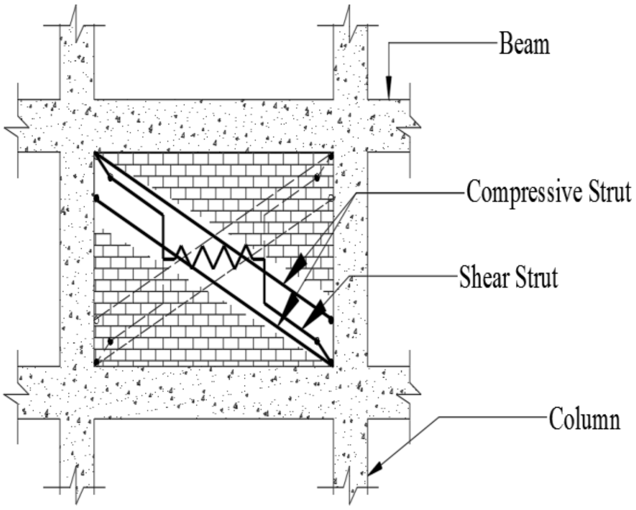

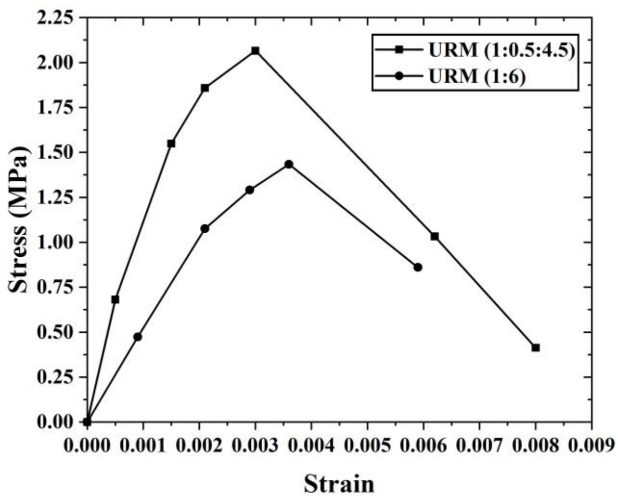

Fig. 2 – Macro-model of infill pannel

Fig. 3 – Compressive stress vs. strain curve of URM prism

2.2 Pushover Analysis

Pushover analysis was performed on the modeled buildings for all the cases considered. The torsional response of buildings is obtained from Extended N2 method (Ex N2) and Extended Capacity Spectrum Method-FEMA 440 (Ex CSM) [15,16]. The seismic performance of the buildings is verified under two levels of ground motion intensity i.e., 0.24g, 0.36g. The ground motion demand is defined in the form of a smooth spectrum. Residual strength is set to 20% of the strength corresponding to ultimate curvature. Gravity loads (1.0*DL*+0.25*LL*) are applied before the application of pushover loads. The lateral load profile chosen for pushover analysis reflects an inverted triangular loading pattern, with the magnitude of loads increasing progressively from bottom to top. The slab-beam interaction is accounted for by modeling the beams with flanges of appropriate width. The geometric nonlinearity effect is neglected.

3. Results and Discussion

Pushover analysis of buildings with and without VSI is carried out under a fixed loading pattern, and the capacity curve for each building in each principal direction is thus obtained. Pushover curves for a few selected buildings are shown in Fig.4. From Fig.4, the following observations can be made which apply to the remaining buildings in both plan directions.

Firstly, in the absence of infill wall, the lateral stiffness and strength characteristics of building with and without VSI are found to be similar. But a sharp distinction in stiffness and strength of these buildings is seen when the infill wall interaction is considered. With an increase in lateral stiffness, the lateral strength of building without VSI is found to be higher compared to building with VSI. Overall lateral displacement capacity of the buildings with infill walls is less compared to without infill wall buildings. This reduction in lateral displacement capacity is associated with a significant drop in the lateral strength and stiffness of the buildings with infill walls. These observations indicate that the energy dissipation capacity of infill wall building is significantly different from bare frame building.

The capacity curve of building in each principal direction is chosen, and target displacement corresponding to the required level of ground motion intensity is calculated. The response of buildings under 0.36g ground motion intensity is presented and discussed below.

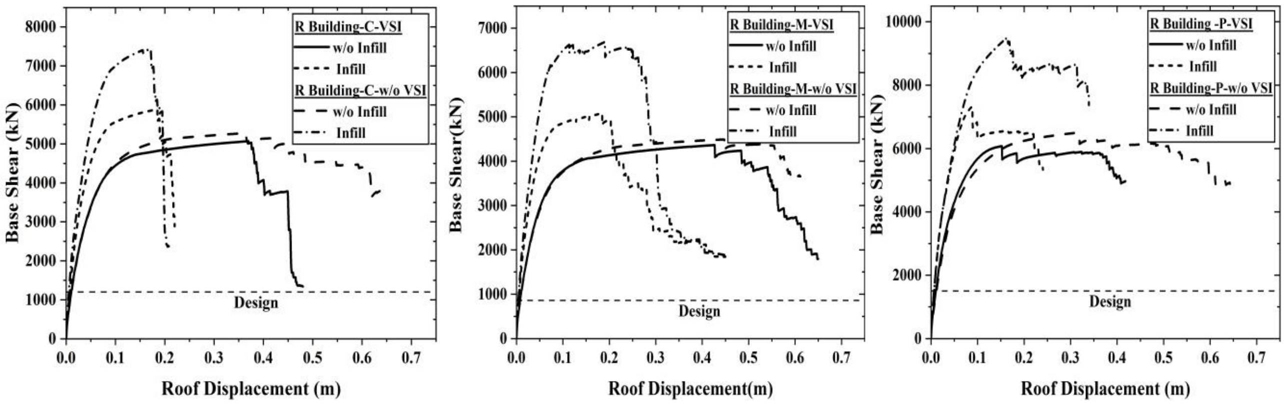

(a) R Building-C (b) R Building-M (c) R Building-4P

Fig. 4 – Pushover curves for the buildings in X- direction.

3.1 Story Drift Ratio (SDR)

The story drift ratio at the stiff, flexible side of the buildings is shown in Fig.5. The SDR between with and without VSI buildings is compared at the level of the first story where combined irregularities are present. Also, the influence of infill wall interaction on the torsional response of the buildings is discussed.

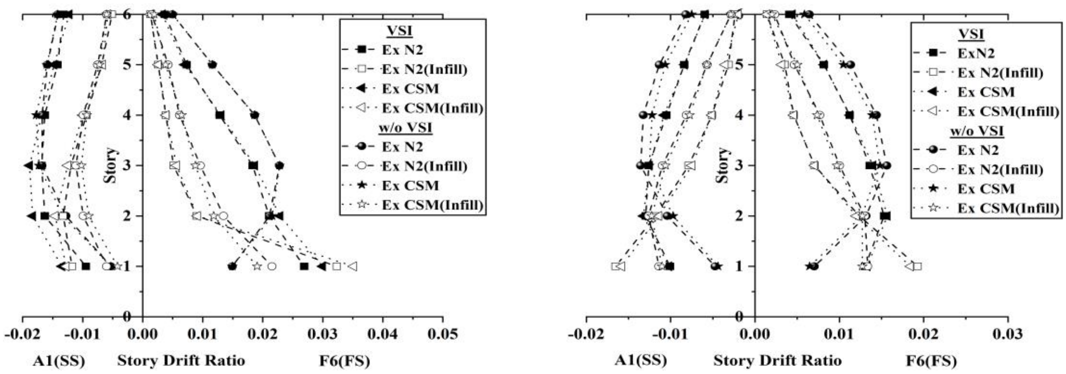

(a) L Building – X (b) L Building – Y

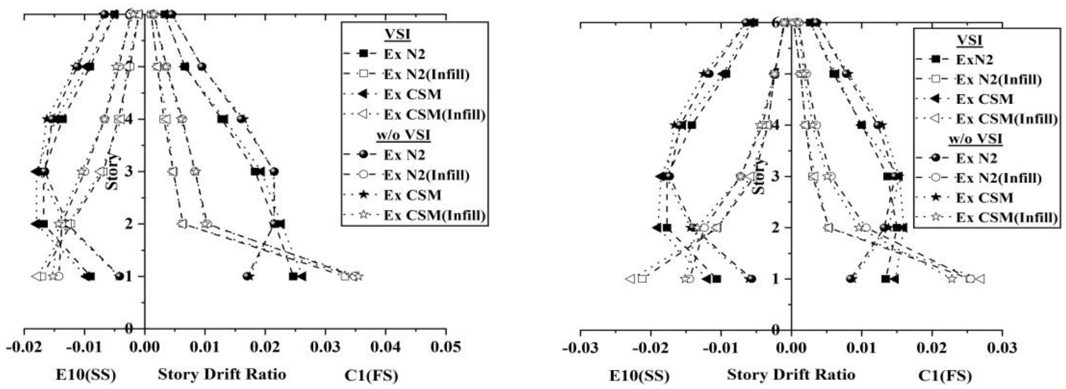

(c) T Building – X (d) T Building – Y

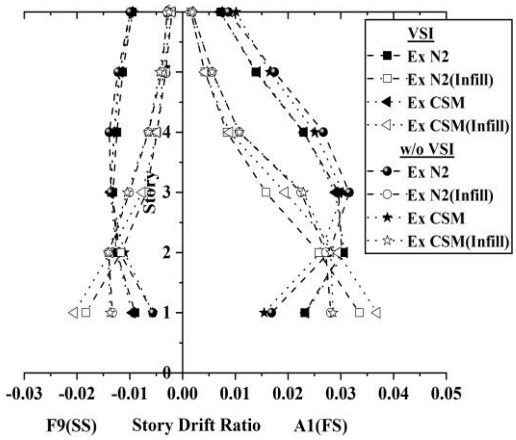

(e) U Building – X

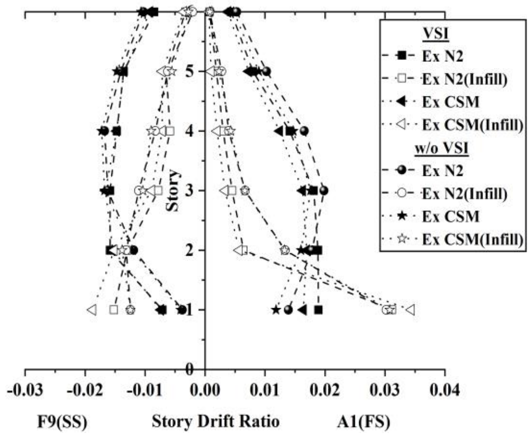

(f) U Building – Y

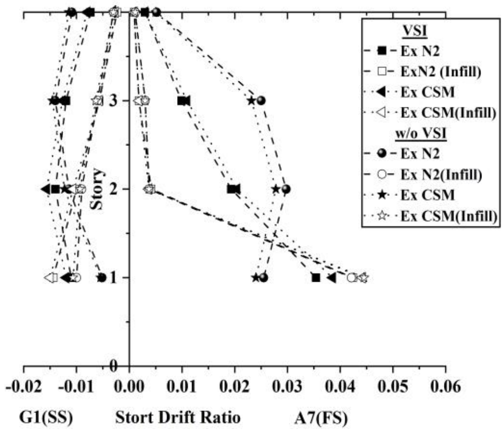

(g) R Building-3P – X

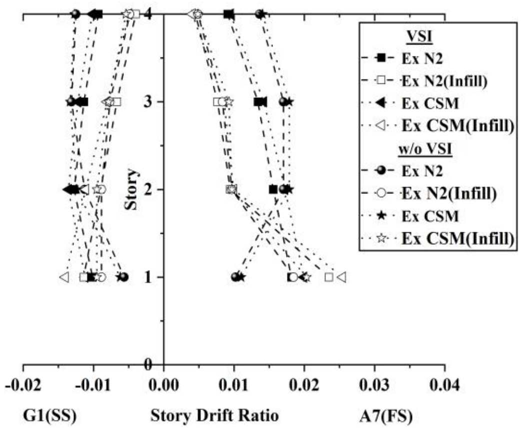

(h) R Building-3P – Y

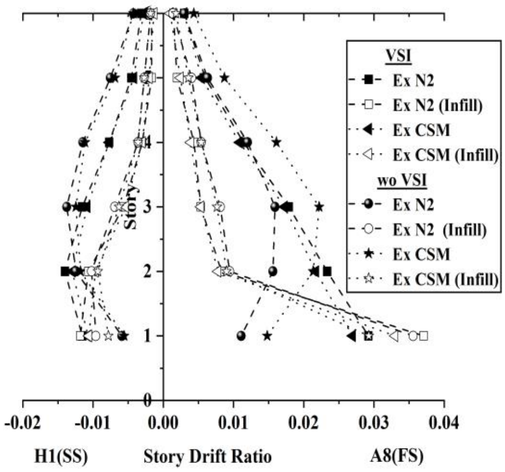

(i) R Building-C – X

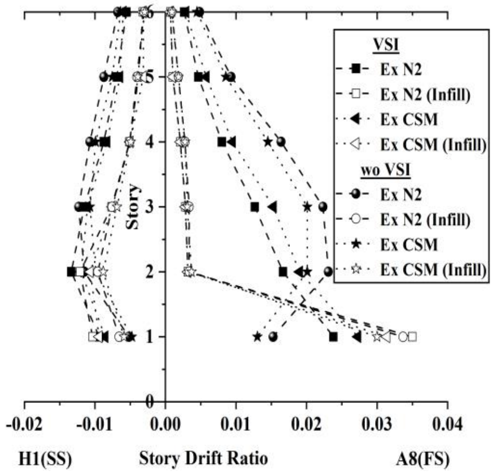

(j) R Building-C – Y

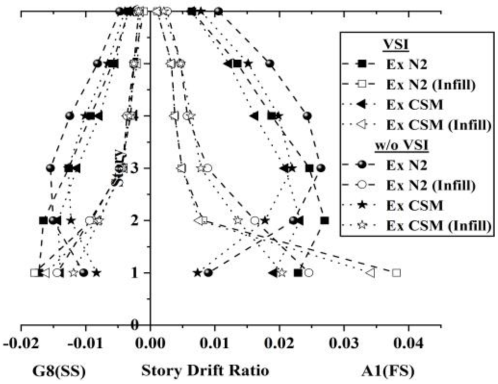

(k) R Building-M – X

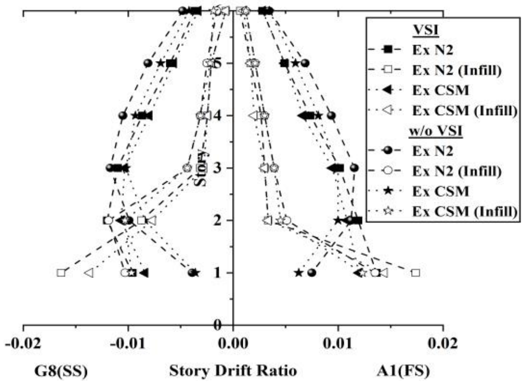

(l) R Building-M – Y

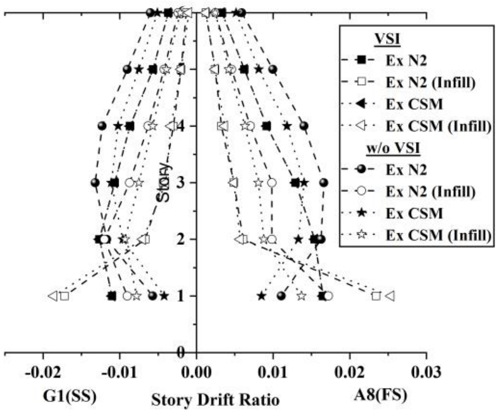

(m) R Building-4P – X

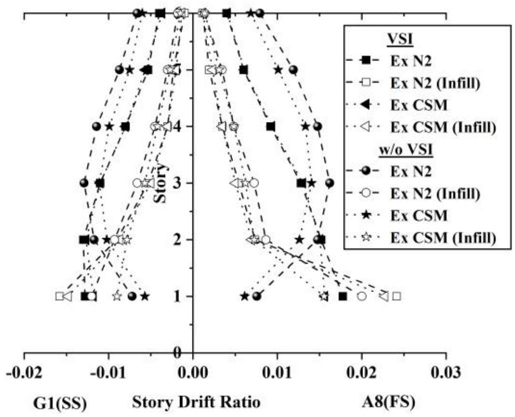

(n) R Building-4P – Y

Fig. 5 – Story Drift Ratio at the stiff(SS), flexible side(FS) of the buildings in X, Y directions

Vertical stiffness irregularity has led to an increase in SDR at stiff, flexible sides of the buildings compared to buildings without VSI as seen in Figs.5(a)-(n) at the bottom story. A similar trend in the SDR values of the story adjacent to a soft first story can be observed, but the increase is not significant. The SDR values of infill wall buildings are found to be higher at the bottom story and decreasing progressively towards the height of the building compared to without infill wall case. Further explanation among the SDR values of with and w/o infill wall buildings is carried out by classifying the buildings based on uncoupled torsional to lateral frequency ratio Ω $(\omega_\theta /\omega_x, \omega_\theta/\omega_y)$. Based on this ratio, L shape, Rectangular-3P, Rectangular-4P buildings are classified as torsionally stiff $(\Omega > 1)$ and T shape building as torsionally flexible $(\Omega < 1)$ in both plan directions. U-shape, Rectangular-M buildings are torsionally stiff in x-direction and torsionally flexible in y-direction. For Rectangular–C building, the first three modes are predominantly torsional.

From Figs.5(a), 5(g), and 5(m) at the bottom story, the SDR values near the flexible side are found to be higher than at the stiff side due to combined irregularities. In Fig.5(a) at the flexible side, SDR values of VSI, w/o VSI buildings are 0.027 and 0.015, respectively. These values are 0.032, 0.021 for similar buildings with infill walls. In Fig.5(m), a similar variation in the SDR values among with and without infill wall buildings is observed. At the flexible side in Fig.5(g), SDR value for VSI, w/o VSI building is 0.035 and 0.025 respectively, whereas this value is 0.042 for both the buildings with infill walls. In y-dir, a difference in SDR values between buildings with and without infill wall is seen, with lesser magnitude compared to the values in x-dir. This change in the response is attributed to the difference in static eccentricity (e_s) and the level of vertical stiffness irregularity (k_1/k_2) among these directions.

For torsionally flexible building, from Figs.5(c), 5(d) the SDR values at the flexible, stiff side are comparable with a higher value for infill wall buildings in both plan directions. In Fig.5(c) for infill wall case, the SDR value is 0.035 for VSI and w/o VSI buildings, which is higher compared to the values 0.025, 0.017 respectively for the same buildings without infill walls.

For U-shape, Rectangular-M building a combination of the above torsionally stiff and flexible behavior is observed. In Figs.5(e), 5(k) higher SDR values are observed at the flexible side in torsionally stiff direction (x-dir). From Figs.5(f), 5(l), the SDR values are comparable at the stiff, flexible side in torsionally flexible direction(y-dir). Figs.5(e)-5(f), 5(k)-5(l) also indicate higher SDR values at the stiff, flexible side for infill wall buildings though the difference in SDR value among VSI and w/o VSI buildings is minimal.

In the case of building with predominant torsional mode, the influence of VSI is seen clearly at the flexible side of the building. As shown in Figs.5(i), 5(j) flexible side experienced higher displacement compared to the stiff side in with and without infill wall buildings.

In summary, the effect of VSI is seen to amplify the torsional response of the story, where vertical and plan irregularity exists together. This amplification is due to the less torsional stiffness of the soft first story compared to a regular story. In the majority of the cases, SDR values at the stiff, flexible side of buildings with infills are higher compared to without infill wall buildings. This increase is due to the abrupt change in lateral stiffness of the bottom story upon consideration of infill walls in the above stories.

3.2 Demand/Capacity Ratio

The D/C ratio of columns located at the stiff, flexible side of the buildings is plotted in Fig.6. The axial load and bending moment values acting on the columns are taken corresponding to the peak value of roof displacement for a ground motion intensity of 0.36g. Results from Ex N2 method are presented, and these ratios are shown for columns located at the first story.

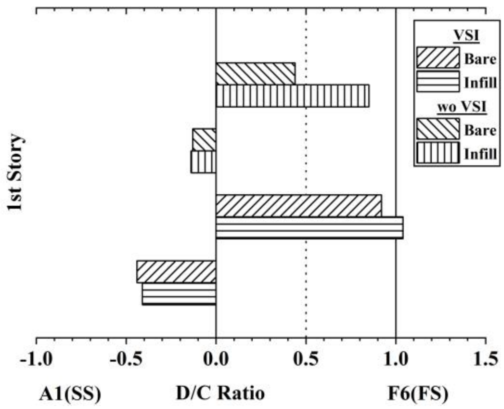

(a) L Building – X

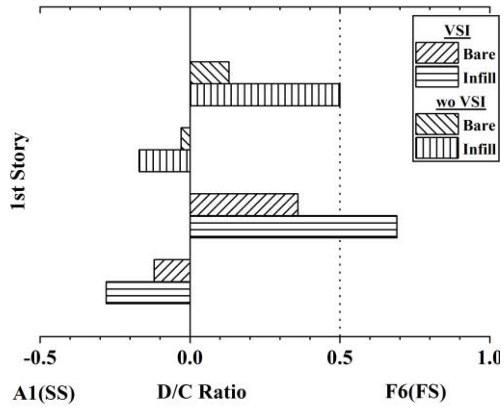

(b) L Building – Y

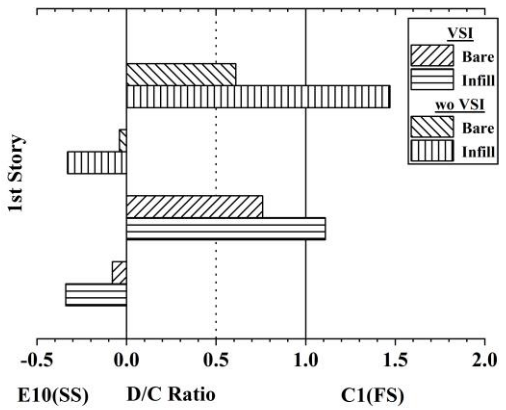

(c) T Building – X

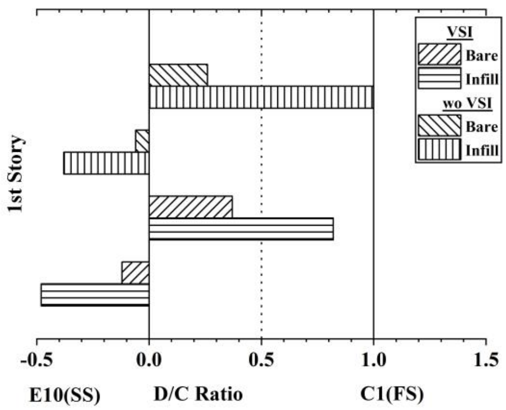

(d) T Building – Y

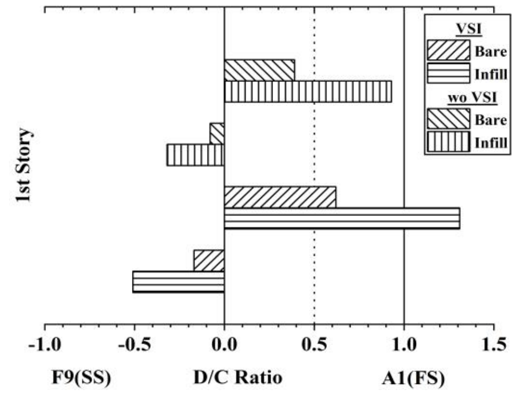

(e) U Building – X

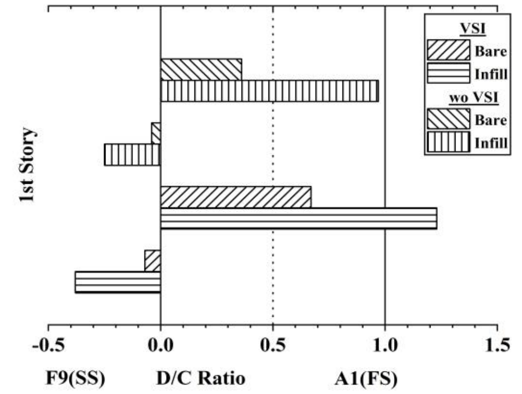

(f) U Building – Y

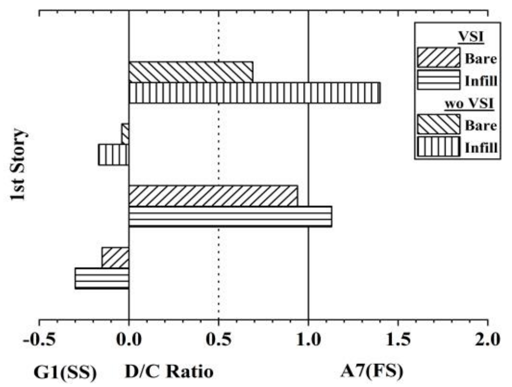

(g) R Building-3P– X

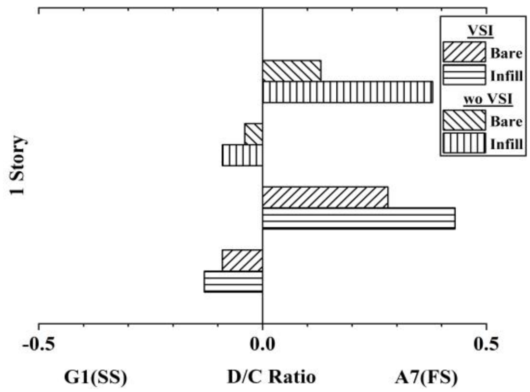

(h) R Building-3P – Y

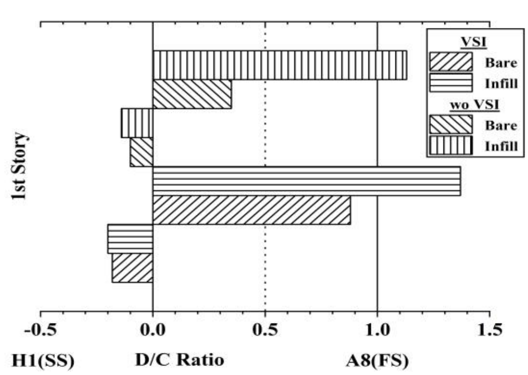

(i) R Building-C– X

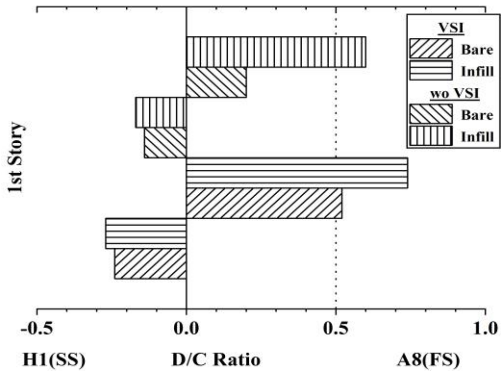

(j) R Building-C – Y

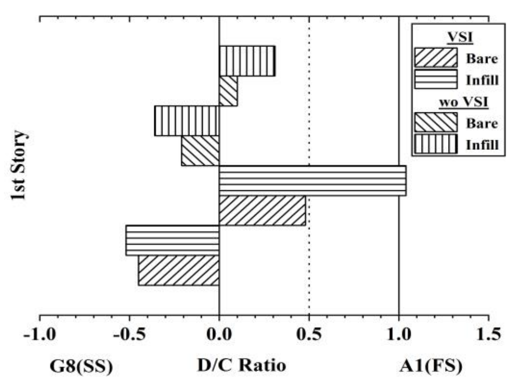

(k) R Building-M– X

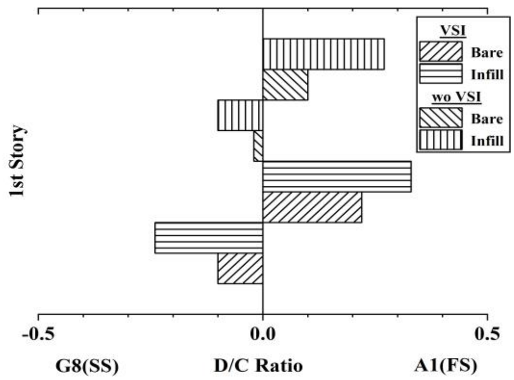

(l) R Building-M – Y

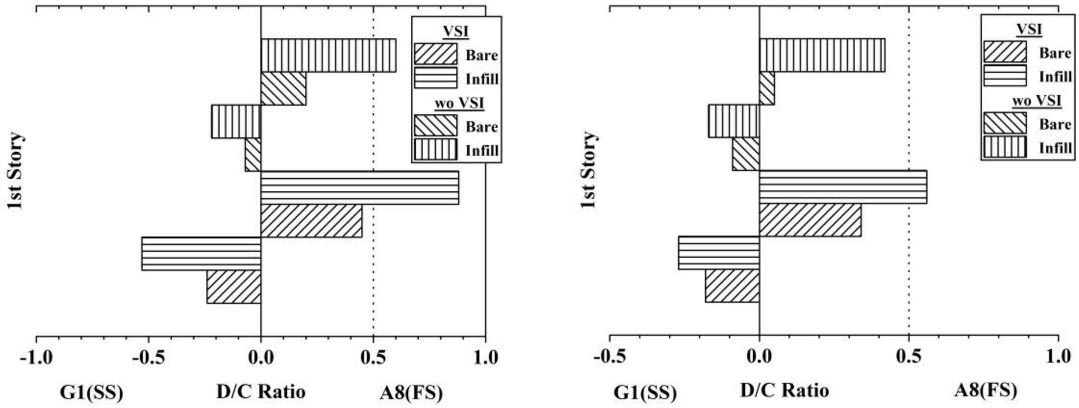

(m) R Building-4P– X (n) R Building-4P – Y

Fig. 6 – Demand to Capacity curvature ratio at the stiff, flexible side of the buildings.

In the majority of the cases, the D/C ratio of the column located at the stiff, flexible side of the VSI building is higher than that of the column located in building w/o VSI. For buildings with infill walls, the D/C ratio of columns is higher compared to without infill wall buildings. Near the stiff side of buildings, the maximum value of the D/C ratio is 0.5 among all the cases.

In the case of torsionally stiff buildings, Figs.6(a), 6(g) reveal that for flexible side column D/C ratio is close to 1.0 except in Fig.6(m) for R Building-4P where this ratio is less than 0.5. In y-dir, the D/C ratio is less than 0.5 for the flexible side column. For the same category of buildings with infills, this ratio is equal to 1.0 or higher in x-dir and 0.5 in y-dir. This variation indicates that force demands on the columns of infill wall buildings are higher compared to without infill wall buildings. Even in the case of a torsionally flexible building, Figs.6(c), 6(d) shows a higher D/C Ratio for the flexible side column, with a value equal to 1 for infill wall case. In both categories of the torsionally stiff and flexible building with infills, the D/C ratio of a column at the flexible side is slightly higher for VSI building compared to building w/o VSI. This observation also holds for building with predominant torsional mode from Figs.6(i), 6(j). This study indicates that the flexible side column of VSI building with infill wall is more vulnerable to crushing failure of confined concrete, especially when D/C > 1. A similar type of failure is noticed for the flexible side column of w/o VSI building when infill wall interaction is considered, which is not the case for similar building without infill wall.

4. Conclusion

The effect of vertical stiffness irregularity on the torsional response of plan asymmetric multistory RC buildings is studied. The torsional response obtained pushover analysis is discussed in terms of story drift ratio and demand to capacity ratio of columns at the stiff, flexible side of the buildings. Also, the effect of infill wall interaction on the torsional response of plan asymmetric buildings is presented, where infill walls are uniformly distributed in plan.

1. Vertical stiffness irregularity leads to amplification of the torsional response of the buildings, with the flexible side column experiencing significant displacement and curvature demand.

2. Infill wall interaction results in modification of torsional response by increasing the vulnerability of the flexible side column to damage in vertically regular and irregular buildings.

The above conclusions are based on the results of pushover analysis only. Further verification of these results has to be carried out by evaluating the response of the buildings from nonlinear time history analysis. This study will be extended further to verify the torsional response of similar buildings with an asymmetric distribution of infill walls in the plan.

5. References

[1] Ouazir, M., Kassoul, A., Ouazir, A., & Achour, B. (2018). Inelastic seismic response of torsionally unbalanced structures with soft first story. *Asian Journal of Civil Engineering*, **19**(5), 571–581.

[2] Fardis, M. N., Bousias, S. N., Franchioni, G., & Panagiotakos, T. B. (1999). Seismic response and design of RC structures with plan-eccentric masonry infills. *Earthquake Engineering and Structural Dynamics*, **28**(2), 173–191.

[3] Kostinakis, K., & Athanatopoulou, A. (2019). Effects of in-plan irregularities caused by masonry infills on the seismic behavior of R/C buildings. *Soil Dynamics and Earthquake Engineering*, **129**, 1–14.

[4] Sai, T. S., Rao, T. C., & Vasudev, B. (2016). Seismic response of RC framed structures having plan and vertical irregularities with and without masonry infill action. *International Research Journal of Engineering and Technology (IRJET)*, **03**(02), 500–513.

[5] Mahdi, T., & Bahreini, V. (2008). Pushover analysis of asymmetrical infilled concrete frames. In *15th World Conference on Earthquake Engineering, Lisbon, Portugal.*

[6] IS1893. (2016). *Criteria for Earthquake Resistant Design of Structures: Part 1 General Provisions and Buildings*. NewDelhi: Bureau of Indian Standards.

[7] SeismoStruct 2016 – A Computer Software for Static and Dynamic Nonlinear Analysis of Framed Structures, ver. 7. *Available from http://www.seismosoft.com.*

[8] Mander, J. B., Priestley, M. J. N., & Park, R. (1989). Theoretical stress-strain model for confined concrete. *Journal of Structural Engineering, ASCE*, **114**(8), 1804–1826.

[9] Monti, G., & Nuti, C. (1992). Nonlinear cyclic behavior of reinforcing bars including buckling. *Journal of Structural Engineering, ASCE*, **118**(12), 3268–3284.

[10] CONSEC©(2017), http://www.structware.com/consec/consec_home.html

[11] Paulay, T., & Priestley, M. J. N. (1992). *Seismic design of reinforced concrete and masonry buildings*. Wiley, New York.

[12] Pinho, R., Bhatt, C., Antoniou, S., & Bento, R. (2008). Modelling of the horizontal slab of a 3D irregular building for nonlinear static assessment. *14th World Conference on Earthquake Engineering, Beijing, China.*

[13] Crisafulli, F. J., & Carr, A. J. (2007). Proposed macro-model for the analysis of infilled frame structures. *Bulletin of the New Zealand Society for Earthquake Engineering*, **40**(2), 69–77.

[14] Kaushik, H. B., Rai, D. C., & Jain, S. K. (2007). Stress-strain characteristics of clay brick masonry under uniaxial compression. *Journal of Materials in Civil Engineering*, **19**(9), 728–739.

[15] Fajfar, P., Marušić, D., & Peruš, I. (2005). Torsional effects in the pushover-based seismic analysis of buildings. *Journal of Earthquake Engineering*, **9**(6), 831–854.

[16] Bhatt, C., & Bento, R. (2011). Extension of the CSM-FEMA440 to plan-asymmetric real building structures. *Earthquake Engineering & Structural Dynamics*, **40**(11), 1263–1282.

